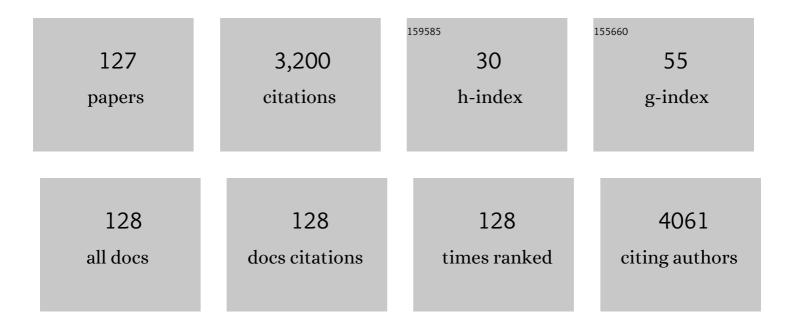
## **Pauls Stradins**

List of Publications by Year in descending order

Source: https://exaly.com/author-pdf/3867267/publications.pdf Version: 2024-02-01



DALLIS STRADINS

#	Article	IF	CITATIONS
1	Van der Waals metal-semiconductor junction: Weak Fermi level pinning enables effective tuning of Schottky barrier. Science Advances, 2016, 2, e1600069.	10.3	446
2	Efficient black silicon solar cell with a density-graded nanoporous surface: Optical properties, performance limitations, and design rules. Applied Physics Letters, 2009, 95, .	3.3	286
3	Nanostructured black silicon and the optical reflectance of graded-density surfaces. Applied Physics Letters, 2009, 94, .	3.3	280
4	Polycrystalline silicon passivated tunneling contacts for high efficiency silicon solar cells. Journal of Materials Research, 2016, 31, 671-681.	2.6	133
5	Realization of GaInP/Si Dual-Junction Solar Cells With 29.8% 1-Sun Efficiency. IEEE Journal of Photovoltaics, 2016, 6, 1012-1019.	2.5	114
6	Progress Towards a 30% Efficient GaInP/Si Tandem Solar Cell. Energy Procedia, 2015, 77, 464-469.	1.8	87
7	Air Passivation of Chalcogen Vacancies in Twoâ€Đimensional Semiconductors. Angewandte Chemie - International Edition, 2016, 55, 965-968.	13.8	80
8	Hydrogen passivation of poly-Si/SiOx contacts for Si solar cells using Al2O3 studied with deuterium. Applied Physics Letters, 2018, 112, .	3.3	80
9	Reformulation of solar cell physics to facilitate experimental separation of recombination pathways. Applied Physics Letters, 2013, 103, .	3.3	78
10	Charge carrier transport mechanisms of passivating contacts studied by temperature-dependent J-V measurements. Solar Energy Materials and Solar Cells, 2018, 178, 15-19.	6.2	78
11	Matrix-embedded silicon quantum dots for photovoltaic applications: a theoretical study of critical factors. Energy and Environmental Science, 2011, 4, 2546.	30.8	72
12	Maximizing tandem solar cell power extraction using a three-terminal design. Sustainable Energy and Fuels, 2018, 2, 1141-1147.	4.9	67
13	Tunnel oxide passivated contacts formed by ion implantation for applications in silicon solar cells. Journal of Applied Physics, 2015, 118, .	2.5	65
14	Strained Interface Defects in Silicon Nanocrystals. Advanced Functional Materials, 2012, 22, 3223-3232.	14.9	63
15	Quasi-Direct Optical Transitions in Silicon Nanocrystals with Intensity Exceeding the Bulk. Nano Letters, 2016, 16, 1583-1589.	9.1	62
16	Effect of silicon oxide thickness on polysilicon based passivated contacts for high-efficiency crystalline silicon solar cells. Solar Energy Materials and Solar Cells, 2018, 185, 270-276.	6.2	60
17	Tin-Catalyzed Plasma-Assisted Growth of Silicon Nanowires. Journal of Physical Chemistry C, 2011, 115, 3833-3839.	3.1	54
18	On the hydrogenation of Poly-Si passivating contacts by Al2O3 and SiN thin films. Solar Energy Materials and Solar Cells, 2020, 215, 110592.	6.2	53

#	Article	IF	CITATIONS
19	Growth of antiphase-domain-free GaP on Si substrates by metalorganic chemical vapor deposition using an <i>in situ</i> AsH3 surface preparation. Applied Physics Letters, 2015, 107, .	3.3	51
20	In Situ Gas-Phase Hydrosilylation of Plasma-Synthesized Silicon Nanocrystals. ACS Applied Materials & Interfaces, 2011, 3, 3033-3041.	8.0	50
21	Three-terminal III–V/Si tandem solar cells enabled by a transparent conductive adhesive. Sustainable Energy and Fuels, 2020, 4, 549-558.	4.9	46
22	Material quality requirements for efficient epitaxial film silicon solar cells. Applied Physics Letters, 2010, 96, 073502.	3.3	43
23	Understanding the charge transport mechanisms through ultrathin SiO <i>x</i> layers in passivated contacts for high-efficiency silicon solar cells. Applied Physics Letters, 2019, 114, .	3.3	41
24	Enhanced Interfacial Stability of Si Anodes for Li-Ion Batteries via Surface SiO <sub>2</sub> Coating. ACS Applied Energy Materials, 2020, 3, 8842-8849.	5.1	38
25	Low-cost plasma immersion ion implantation doping for Interdigitated back passivated contact (IBPC) solar cells. Solar Energy Materials and Solar Cells, 2016, 158, 68-76.	6.2	37
26	Surface SiO <sub>2</sub> Thickness Controls Uniform-to-Localized Transition in Lithiation of Silicon Anodes for Lithium-Ion Batteries. ACS Applied Materials & amp; Interfaces, 2020, 12, 27017-27028.	8.0	37
27	Interdigitated Back Passivated Contact (IBPC) Solar Cells Formed by Ion Implantation. IEEE Journal of Photovoltaics, 2016, 6, 41-47.	2.5	36
28	Light trapping by a dielectric nanoparticle back reflector in film silicon solar cells. Applied Physics Letters, 2011, 99, 064101.	3.3	34
29	Equivalent Performance in Three-Terminal and Four-Terminal Tandem Solar Cells. IEEE Journal of Photovoltaics, 2018, 8, 1584-1589.	2.5	31
30	Backâ€contacted bottom cells with three terminals: Maximizing power extraction from currentâ€mismatched tandem cells. Progress in Photovoltaics: Research and Applications, 2019, 27, 410-423.	8.1	31
31	Significant improvement in silicon chemical vapor deposition epitaxy above the surface dehydrogenation temperature. Journal of Applied Physics, 2006, 100, 093520.	2.5	29
32	Effect of Crystallographic Orientation and Nanoscale Surface Morphology on Poly-Si/SiO <sub><i>x</i></sub> Contacts for Silicon Solar Cells. ACS Applied Materials & Interfaces, 2019, 11, 42021-42031.	8.0	29
33	Effect of Water Concentration in LiPF <sub>6</sub> -Based Electrolytes on the Formation, Evolution, and Properties of the Solid Electrolyte Interphase on Si Anodes. ACS Applied Materials & Interfaces, 2020, 12, 49563-49573.	8.0	27
34	Transparent Conductive Adhesives for Tandem Solar Cells Using Polymer–Particle Composites. ACS Applied Materials & Interfaces, 2018, 10, 8086-8091.	8.0	25
35	Effect of the SiO2 interlayer properties with solid-source hydrogenation on passivated contact performance and surface passivation. Energy Procedia, 2017, 124, 295-301.	1.8	24
36	Mechanisms controlling the phase and dislocation density in epitaxial silicon films grown from silane below 800 A°C. Applied Physics Letters, 2010, 96, .	3.3	23

#	Article	IF	CITATIONS
37	Probing the Evolution of Surface Chemistry at the Silicon–Electrolyte Interphase via In Situ Surface-Enhanced Raman Spectroscopy. Journal of Physical Chemistry Letters, 2020, 11, 286-291.	4.6	23
38	A new real-time quantum efficiency measurement system. Conference Record of the IEEE Photovoltaic Specialists Conference, 2008, , .	0.0	18
39	Growth of amorphous and epitaxial ZnSiP <sub>2</sub> –Si alloys on Si. Journal of Materials Chemistry C, 2018, 6, 2696-2703.	5.5	18
40	Effect of Surface Texture on Pinhole Formation in SiO <i><sub>x</sub></i> -Based Passivated Contacts for High-Performance Silicon Solar Cells. ACS Applied Materials & Interfaces, 2020, 12, 55737-55745.	8.0	18
41	Reactive ion etched, self-aligned, selective area poly-Si/SiO2 passivated contacts. Solar Energy Materials and Solar Cells, 2020, 217, 110621.	6.2	18
42	Anneal treatment to reduce the creation rate of light-induced metastable defects in device-quality hydrogenated amorphous silicon. Applied Physics Letters, 2011, 98, 201908.	3.3	17
43	Cone kinetics model for two-phase film silicon deposition. Applied Physics Letters, 2008, 92, 093114.	3.3	15
44	Free standing silica thin films with highly ordered perpendicular nanopores. RSC Advances, 2014, 4, 7627-7633.	3.6	15
45	Air Passivation of Chalcogen Vacancies in Twoâ€Dimensional Semiconductors. Angewandte Chemie, 2016, 128, 977-980.	2.0	15
46	Modifications of Textured Silicon Surface Morphology and Its Effect on Poly-Si/SiO <i> <sub>x</sub> </i> Contact Passivation for Silicon Solar Cells. IEEE Journal of Photovoltaics, 2019, 9, 1513-1521.	2.5	13
47	Outdoor performance of a tandem InGaP/Si photovoltaic luminescent solar concentrator. Solar Energy Materials and Solar Cells, 2021, 223, 110945.	6.2	13
48	Solid phase crystallization of hot-wire CVD amorphous silicon films. Materials Research Society Symposia Proceedings, 2005, 862, 1051.	0.1	12
49	Physics and chemistry of hot-wire chemical vapor deposition from silane: Measuring and modeling the silicon epitaxy deposition rate. Journal of Applied Physics, 2010, 107, 054906.	2.5	12
50	<i>Tabula Rasa</i> for <i>n</i> z siliconâ€based photovoltaics. Progress in Photovoltaics: Research and Applications, 2019, 27, 136-143.	8.1	12
51	Isolating p- and n-Doped Fingers With Intrinsic Poly-Si in Passivated Interdigitated Back Contact Silicon Solar Cells. IEEE Journal of Photovoltaics, 2020, 10, 1574-1581.	2.5	12
52	Self-Aligned Selective Area Front Contacts on <i>Poly</i> -Si/SiO <i> <sub>x</sub> </i> Passivating Contact <i>c</i> -Si Solar Cells. IEEE Journal of Photovoltaics, 2022, 12, 678-689.	2.5	10
53	Comparison of thin epitaxial film silicon photovoltaics fabricated on monocrystalline and polycrystalline seed layers on glass. Progress in Photovoltaics: Research and Applications, 2015, 23, 909-917.	8.1	9
54	Measurement of poly-Si film thickness on textured surfaces by X-ray diffraction in poly-Si/SiO passivating contacts for monocrystalline Si solar cells. Solar Energy Materials and Solar Cells, 2022, 236, 111510.	6.2	9

#	Article	IF	CITATIONS
55	Real Time Monitoring of the Crystallization of Hydrogenated Amorphous Silicon. Materials Research Society Symposia Proceedings, 2005, 862, 1611.	0.1	8
56	Epitaxial crystal silicon absorber layers and solar cells grown at 1.8 microns per minute. , 2011, , .		8
57	Device Physics of Heteroepitaxial Film c-Si Heterojunction Solar Cells. IEEE Journal of Photovoltaics, 2013, 3, 230-235.	2.5	8
58	Indium zinc oxide mediated wafer bonding for IIIâ $\in$ "V/Si tandem solar cells. , 2015, , .		8
59	Trap-Assisted Dopant Compensation Prevents Shunting in Poly-Si Passivating Interdigitated Back Contact Silicon Solar Cells. ACS Applied Energy Materials, 2021, 4, 10774-10782.	5.1	8
60	Staebler-Wronski defects: Creation efficiency, stability, and effect on a-Si:H solar cell degradation. , 2010, , .		7
61	Tunneling or Pinholes: Understanding the Transport Mechanisms in SiO <inf>x</inf> Based Passivated Contacts for High-Efficiency Silicon Solar Cells. , 2018, , .		7
62	Comparative Study of Solid-Phase Crystallization of Amorphous Silicon Deposited by Hot-wire CVD, Plasma-Enhanced CVD, and Electron-Beam Evaporation. Materials Research Society Symposia Proceedings, 2007, 989, 4.	0.1	6
63	Dislocation-limited open circuit voltage in film crystal silicon solar cells. Applied Physics Letters, 2012, 101, 123510.	3.3	6
64	Selective area growth of GaAs on Si patterned using nanoimprint lithography. , 2016, , .		6
65	Atomic structure of light-induced efficiency-degrading defects in boron-doped Czochralski silicon solar cells. Energy and Environmental Science, 2021, 14, 5416-5422.	30.8	6
66	Chemical Passivation of Crystalline Si by Al <sub>2</sub> O <sub>3</sub> Deposited Using Atomic Layer Deposition: Implications for Solar Cells. ACS Applied Nano Materials, 2021, 4, 6629-6636.	5.0	6
67	Transparent Conductive Adhesives for Tandem Solar Cells. , 2017, , .		5
68	600 mV epitaxial crystal silicon solar cells grown on seeded glass. , 2013, , .		4
69	Study of nickel silicide as a copper diffusion barrier in monocrystalline silicon solar cells. , 2016, , .		4
70	Operating principles of three-terminal solar cells. , 2018, , .		4
71	Influence of Tabula Rasa on Process- and Light-Induced Degradation of Solar Cells Fabricated From Czochralski Silicon. IEEE Journal of Photovoltaics, 2020, 10, 1557-1565.	2.5	4
72	Junction transport in epitaxial film silicon heterojunction solar cells. , 2011, , .		3

#	Article	IF	CITATIONS
73	Bulk defect generation during B-diffusion and oxidation of CZ wafers: Mechanism for degrading solar cell performance. , 2014, , .		3
74	Ion implanted passivated contacts for interdigitated back contacted solar cells. , 2015, , .		3
75	Atomic scale understanding of poly-Si/SiO <inf>2</inf> /c-Si passivated contacts: Passivation degradation due to metallization. , 2016, , .		3
76	Accelerated reliability tests of n+ and p+ poly-Si passivated contacts. Solar Energy Materials and Solar Cells, 2022, 236, 111469.	6.2	3
77	Area-Dependent Switching in Thin Film-Silicon Devices. Materials Research Society Symposia Proceedings, 2003, 762, 1831.	0.1	2
78	Physics of Solid-Phase Epitaxy of Hydrogenated Amorphous Silicon for Thin Film Si Photovoltaics. Materials Research Society Symposia Proceedings, 2006, 910, 5.	0.1	2
79	Synthesis and characterization of PECVD-grown, silane-terminated silicon quantum dots. , 2012, , .		2
80	Energy conversion properties of ZnSiP <inf>2</inf> , a lattice-matched material for silicon-based tandem photovoltaics. , 2016, , .		2
81	Nonisovalent Si-III-V and Si-II-VI alloys: Covalent, ionic, and mixed phases. Physical Review B, 2017, 96, .	3.2	2
82	Yield analysis and comparison of GaInP/Si and GaInP/GaAs multi-terminal tandem solar cells. AIP Conference Proceedings, 2018, , .	0.4	2
83	Critical interface: Poly-silicon to tunneling SiO2 for passivated contact performance. AIP Conference Proceedings, 2019, , .	0.4	2
84	III-V/Si Tandem Cells Utilizing Interdigitated Back Contact Si Cells and Varying Terminal Configurations. , 2019, , .		2
85	Quality and Growth Rate of Hot-wire Chemical Vapor Deposition Epitaxial Si Layers. Materials Research Society Symposia Proceedings, 2008, 1066, 1.	0.1	1
86	Metastable Defects in Light Soaked Amorphous Silicon at 77 K. Materials Research Society Symposia Proceedings, 2008, 1066, 1.	0.1	1
87	Phase evolution in nanocrystalline silicon films: Hydrogen dilution and the cone kinetics model. Philosophical Magazine, 2009, 89, 2461-2468.	1.6	1
88	Device physics of heteroepitaxial film c-Si heterojunction solar cells. , 2012, , .		1
89	Improved 750 °C epitaxial crystal silicon solar cells through impurity reduction. , 2013, , .		1
90	Study of the passivation mechanism of c-Si by Al <inf>2</inf> O <inf>3</inf> using in situ infrared		1

spectroscopy., 2014, , .

#	Article	IF	CITATIONS
91	Plasma immersion ion implantation for interdigitated back passivated contact (IBPC) solar cells. , 2016, , .		1
92	Bandgap and carrier transport engineering of quantum confined mixed phase nanocrystalline/amorphous silicon. , 2016, , .		1
93	III-V/Si tandem cell to module interconnection - comparison between different operation modes. , 2017, , ,		1
94	Modeling three-terminal III- V ISi tandem solar cells. , 2017, , .		1
95	Self-Aligned, Selective Area Poly-Si/SiO <sub>2</sub> Passivated Contacts for Enhanced Photocurrent in Front/Back Solar Cells. , 2019, , .		1
96	Nonuniform Charge Collection in SiO <sub>x</sub> -Based Passivated-Contact Silicon Solar Cells. , 2019, , .		1
97	Spectroscopic Investigation of Light-Induced Degradation Paramagnetic Defect in Czochralski Silicon. , 2020, , .		1
98	Effect of Dopant Compensation on the Conductivity of the Intrinsic poly-Si Isolation Region in Passivated IBC Silicon Solar Cells. , 2020, , .		1
99	Increase of temperature and crystallinity during electrical switching in microcrystalline silicon. Materials Research Society Symposia Proceedings, 2004, 808, 185.	0.1	0
100	Combinatorial Studies of Switching and Solid-Phase Crystallization in Amorphous Silicon. Materials Research Society Symposia Proceedings, 2005, 894, 1.	0.1	0
101	ESR Study of Crystallization of Hydrogenated Amorphous Silicon Thin Films. Materials Research Society Symposia Proceedings, 2007, 989, 13.	0.1	0
102	Metastable Defects in Tritiated Amorphous Silicon. Materials Research Society Symposia Proceedings, 2007, 989, 4.	0.1	0
103	Cone Kinetics Model: Insights into the Morphologies of Mixed-phase Silicon Film Growth. Materials Research Society Symposia Proceedings, 2008, 1066, 1.	0.1	0
104	Photovoltaic-quality silicon epitaxy by hot-wire CVD at glasscompatible temperatures. , 2009, , .		0
105	Epitaxial film silicon solar cells fabricated by hot wire chemical vapor deposition below 750°C. , 2009, , .		0
106	Silicon quantum dot optical properties and synthesis: Implications for photovoltaic devices. , 2010, , .		0
107	Reduced light-induced degradation in a-Si:H: The role of network nanostructure. , 2011, , .		0
108	New analysis of suns-V <inf>oc</inf> and V <inf>oc</inf> (T): A simple method to quantify recombination channels in solar cells. , 2013, , .		0

#	Article	IF	CITATIONS
109	Device physics of heteroepitaxial film c-Si heterojunction solar cells. , 2013, , .		О
110	Dielectric stack passivation on boron- and phosphorus-diffused surfaces and 20% efficient PERT cell on n-CZ silicon substrate. , 2014, , .		0
111	A Novel Method to Investigate Stoichiometry and Performance of Buried Passivated Contacts Utilizing Time-of-Flight SIMS. , 2017, , .		0
112	An Isotope Study of Hydrogen Passivation of poly-Si/SiOx Passivated Contacts for Si Solar Cells. , 2017, , $\cdot$		0
113	Dopant Patterning by PECVD and Mechanical Masking for Passivated Tunneling Contact IBC Cell Architectures. , 2017, , .		0
114	Self Aligned Aluminum Selective Emitter for n-type Si Cells. , 2017, , .		0
115	the Iimplied Voc of Passivated Contacts for c-Si Based Solar Cells. , 2017, , .		Ο
116	Tabula Rasa: Oxygen precipitate dissolution though rapid high temperature processing in silicon. , 2017, , .		0
117	Luminescent Solar Concentrator Tandem-on-Silicon with above 700mV Passivated Contact Silicon Bottom Cell. , 2019, , .		Ο
118	Enhancing Photocarrier Bulk Lifetime with Defect Engineering of Polycrystalline Passivated-Contact n-Cz Photovoltaic Devices. , 2019, , .		0
119	Mitigating Process Induced Degradation in p- and n-Czochralski Silicon Wafers with Tabula Rasa. , 2019, , .		Ο
120	Understanding and Mitigating the Contamination of Intrinsic poly-Si Gaps in Passivated IBC Solar Cells. , 2019, , .		0
121	Effective Dielectric Passivation Scheme in Area-Selective Front/Back Poly-Si/SiOx Passivating Contact Solar Cells. , 2021, , .		Ο
122	Electron Paramagentic Resonance Investigation of Mechanism of Light- and Elevated-Temperature-Induced Degradation in Ga-doped Cz Si. , 2021, , .		0
123	Fabrication of Poly-Si on Locally Etched SiOx as Passivating Contacts for c-Si Solar Cells. , 2021, , .		Ο
124	Trap-Assisted Dopant Compensation Prevents Shunting in poly-Si Passivating Interdigitated Back Contact Silicon Solar Cells. , 2021, , .		0
125	Understanding the origin of Tabula Rasa process-induced defects in CZ n-type c-Si. , 2020, , .		0
126	Submicron Thickness Characterization of poly-Si thin films on Textured Surfaces by X-ray Diffraction for Minimizing Parasitic Absorption in Poly-Si/SiO2 Passivating Contact Cells. , 2020, , .		0

#	Article	IF	CITATIONS
127	Pinhole formation in poly-Si/SiOx passivating contacts on Si(111)-oriented textures. , 2020, , .		0